

Modeling acclimation of photosynthesis to temperature in evergreen conifer forests

Guillermo Gea-Izquierdo¹, Annikki Mäkelä², Hank Margolis³, Yves Bergeron⁴, T. Andrew Black⁵, Allison Dunn⁶, Julian Hadley⁷, Kyaw Tha Paw U⁸, Matthias Falk⁸, Sonia Wharton¹⁵, Russell Monson⁹, David Y. Hollinger¹⁰, Tuomas Laurila¹¹, Mika Aurela¹¹, Harry McCaughey¹², Charles Bourque¹³, Timo Vesala¹⁴ and Frank Berninger¹

¹Centre d'Étude de la Forêt (CEF), Département des Sciences Biologiques, Université du Québec à Montréal, CP 8888 Succ. Centre Ville, Montréal (Qc), H3P 3P8, Canada; ²Department of Forest Ecology, PO Box 27, 00014 University of Helsinki, Finland; ³Centre d'Étude de la Forêt, Faculté de Foresterie, de Géographie et de Géomatique, Université Laval Québec, QC G1V 0A6, Canada; ⁴Université du Québec en Abitibi-Témiscamingue, 445 Boulevard de l'Université, Rouyn-Noranda, QC J9X 5E4, Canada; ⁵The University of British Columbia, Faculty of Land and Food Systems, 2357 Main Mall, Vancouver, BC V6T1Z4, Canada; ⁶Department of Earth & Planetary Sciences, Harvard University, 20 Oxford Street, Cambridge, MA 02138, USA; ⁷Harvard University, Harvard Forest, PO Box 68, 324 N, Main Street, Petersham, MA 01366, USA; ⁸University of California – Davis, Dept of Land, Air and Water Resources, One Shields Avenue, Davis, CA 95616-8627, USA; ⁹University of Colorado, Dept of Ecology and Evolutionary Biology, Campus Box 334, Boulder, CO 80309, USA; ¹⁰USDA Forest Service, Northern Research Station, 271 Mast Rd, Durham, NH 03824, USA; ¹¹Finnish Meteorological Institute, PO Box 503, Helsinki FI-00101, Finland; ¹²Queen's University, Department of Geography, Mackintosh Corry Hall, Room E112, Kingston, Canada K7L 3N6; ¹³University of New Brunswick, Forestry & Environmental Management, 28 Dineen Drive, PO Box 4400, Fredericton, Canada, E3B 5A3; ¹⁴Department of Physics, PO Box 48, FI-00014, University of Helsinki, Helsinki, Finland; ¹⁵Atmospheric, Earth and Energy Division, Lawrence Livermore National Laboratory, 7000 East Avenue, Livermore, CA 94551

Summary

Author for correspondence:

Guillermo Gea-Izquierdo
Tel: +41 44 739 2392
Email: guigeiz@gmail.com,
guillermo.gea@wsl.ch

Received: 4 May 2010
Accepted: 25 May 2010

New Phytologist (2010)
doi: 10.1111/j.1469-8137.2010.03367.x

Key words: boreal ecosystems, carbon fluxes, eddy covariance, mechanistic models, temperature acclimation.

- In this study, we used a canopy photosynthesis model which describes changes in photosynthetic capacity with slow temperature-dependent acclimations.
- A flux-partitioning algorithm was applied to fit the photosynthesis model to net ecosystem exchange data for 12 evergreen coniferous forests from northern temperate and boreal regions.
- The model accounted for much of the variation in photosynthetic production, with modeling efficiencies (mean > 67%) similar to those of more complex models. The parameter describing the rate of acclimation was larger at the northern sites, leading to a slower acclimation of photosynthesis to temperature. The response of the rates of photosynthesis to air temperature in spring was delayed up to several days at the coldest sites. Overall photosynthesis acclimation processes were slower at colder, northern locations than at warmer, more southern, and more maritime sites.
- Consequently, slow changes in photosynthetic capacity were essential to explaining variations of photosynthesis for colder boreal forests (i.e. where acclimation of photosynthesis to temperature was slower), whereas the importance of these processes was minor in warmer conifer evergreen forests.

Introduction

Climate change will affect northern ecosystems by changes in CO₂ concentrations, temperature, and the length of the period when ecosystems are physiologically active. Warmer spring temperatures have advanced the budbreak of many

plant species and satellite imagery confirms that northern areas are generally greening earlier (Myneni *et al.*, 1997). However, this is not evident at all locations, and reductions of forest growth as a consequence of water stress and later snow melt have also been reported in some boreal forests (Vaganov *et al.*, 1999; D'Arrigo *et al.*, 2004). These studies

shed little light on the possible effects of longer growing seasons on the gross primary productivity and carbon (C) balance of evergreen boreal and coniferous northern temperate forests. At some northern evergreen sites (Hollinger *et al.*, 2004), annual net ecosystem C uptake has been found to increase when springtime air temperatures are warmer than normal. For evergreen species, leaf-out dates and other traditional or remotely sensed phenological variables are only of marginal importance for gross primary productivity and C balance of these systems since leaves persist over several years. Nevertheless, it is well known that the photosynthetic capacity of boreal evergreen conifers is greatly diminished in the winter, and the start of photosynthesis in spring requires a reorganization of the photosynthetic apparatus (Ensminger *et al.*, 2004).

Phenological models have long been used to describe traditional phenological variables such as leaf-out or flowering dates (Linkosalo, 1999). These models, which are frequently built on heat sum and day-length approaches, report reasonable predictions of these events. The nature of the start of the photosynthesis in evergreen trees is, however, quite different. Initial photosynthetic capacity seems to be a reversible process (Pelkonen & Hari, 1980) while budburst and leaf development are typically irreversible, and there seems to be a seasonal behavior of photosynthesis in boreal conifers (Thum *et al.*, 2008). Frost hardening and modeling of forest phenology using temperature indices have been shown to be more effective on colder sites in Scandinavia (Thum *et al.*, 2009). To our knowledge, there are no generally accepted models that describe this recovery process and no large-scale analysis has been carried out to understand how factors such as climate, species, or stand structure affect the recovery of photosynthesis.

Good estimates of photosynthesis are required to improve our understanding of ecosystem production and ecosystem C balances under a changing climate. Global carbon models are important tools for managing and predicting ecosystem behavior under future climate scenarios (e.g. Berninger, 1997; Morales *et al.*, 2005; Friend *et al.*, 2007). These models generally consider photosynthesis to respond directly to temperature. However, it is difficult to find unique factors that explain intersite differences in ecosystem productivity as there are many factors affecting photosynthesis.

In this work, we model the C flux of 12 boreal evergreen needle-leaf forests and study the between-site variability of model parameters as a response to temperature and latitude in several locations comprising different ecological situations. The model used was based on Mäkelä *et al.* (1996, 2004), a simple photosynthesis model that focuses on the long-term acclimation of leaf photochemistry to fluctuations in temperature. The relationship between the parameters and differences in latitude, continentality, and stand characteristics is discussed. We specifically address the questions of how to describe changes in the photosynthetic capacity

during periods when the photosystem is acclimating to temporal changes in temperature; and to what extent differences in climate, species or canopy greenness (as measured by the normalized difference vegetation index (NDVI)) are able to account for differences in the parameters of the photosynthesis model.

Materials and Methods

Study sites and data used

The studied datasets included 12 eddy-covariance stations located in boreal evergreen and northern temperate needle-leaf forests from the Fluxnet-Canada Research Network (<http://www.fluxnet-canada.ca>), Fluxnet (<http://www.fluxnet.ornl.gov/fluxnet/siteplan.cfm>), and Ameriflux (<http://public.ornl.gov/ameriflux>). All the flux sites were located at latitudes > 40° in both North America and Europe, including stations with very different precipitation and temperature regimes. We explicitly tried to minimize the effects of stand age on the model results by choosing mature stands to exclude the effects of stand dynamics on fluxes (Goulden *et al.*, 2006). Their main characteristics are shown in Table 1. Fluxes were measured in all cases using the eddy-covariance method (Baldocchi, 2003). Half-hourly eddy flux data were used to calibrate the model. We used site-specific friction velocity thresholds: only data with good mixing conditions and where friction velocity was not correlated with the flux were used in the analyses (Falge *et al.*, 2001; Reichstein *et al.*, 2005). The primary interest of this study is the modeling of the gross ecosystem exchange (GEE) of our forest stands. However, we derived this variable from measurements of net ecosystem exchange (NEE), which are broken down into GEE and ecosystem respiration (R_{eco}). Since R_{eco} was calculated using different algorithms in different datasets, we decided to estimate it ourselves from the data, using the same algorithm for all sites.

Flux models

Net ecosystem exchange was modeled using a flux-partitioning algorithm where $NEE = R_{\text{eco}} - GEE$. All C flux estimates are in $\mu\text{mol m}^{-2} \text{s}^{-1}$ and negative values of NEE correspond to forests acting as C sinks. R_{eco} was modeled following the model of Lloyd & Taylor (1994) assuming an Arrhenius-type relationship with air temperature, using the expression:

$$R_{\text{eco}}(t) = R_{10} \exp \left(308.56 \cdot \left(\frac{1}{56.02} - \left(\frac{1}{(T_{\text{air}}(t) + 46.02)} \right) \right) \right) \quad \text{Eqn 1}$$

where $T_{\text{air}}(t)$ is the measured temperature above the canopy in Celsius at time (t) and R_{10} is the mean respiration at

Table 1 Site characteristics of eddy-covariance data sets used

#	Station	Country	Latitude, longitude	Stand height (m)	Mean stand age	Altitude (m)	Dominant tree species	Period	NEE ($\mu\text{mol m}^{-2} \text{s}^{-1}$)		Climatic data		Reference
									Mean	SD	Annual Prec (mm)	Tmean (°C)	
1	NOBS	Canada	55.9°N, 98.5°W	10.6	150	259	<i>Picea mariana</i> (Mill.) Britton, Sterns & Poggenburg	1994–2006	-0.534	3.163	517.0	-2.9	Dunn et al. (2007)
2	Harvard hemlock	USA	42.5°N, 72.2°W	22	150	360	<i>Tsuga canadensis</i> (L.) Carr.	2000–2004	-1.845	5.729	1102.0	7.5	Hadley & Schedlbauer (2002)
3	Wind River	USA	45.8°N, 122.0°W	60	500	371	<i>Pseudotsuga menziesii</i> (Mirb.) Franco, <i>Tsuga heterophylla</i> (Raf.) Sarg.	1999–2006	-3.410	8.088	2528.0	8.7	Falk et al. (2008)
4	Niwot Ridge	USA	40.0°N, 105.5°W	11.5	100	3050	<i>Abies lasiocarpa</i> (Hooker) Nuttall, <i>Picea engelmannii</i> Parry ex Engelm., <i>Pinus contorta</i> Dougl. ex S.P. Mill.	1998–2007	-0.181	3.329	800.0	1.5	Monson et al. (2002)
5	Howland Forest	USA	45.2°N, 68.7°W	20	109	79	<i>Picea rubens</i> Sarg., <i>Tsuga canadensis</i> (L.) Carr., <i>Abies balsamea</i> (L.) Mill., <i>Pinus strobus</i> L., <i>Thuja occidentalis</i> (L.) Mill.	1996–2004	-2.457	6.349	777.5	6.7	Hollinger et al. (1999)
6	Sask-Black Spruce	Canada	54.0°N, 105.1°W	14	125	597	<i>Picea mariana</i> (Mill.) Britton, Sterns & Poggenburg	1999–2005	-1.061	3.409	405.6	0.8	Black et al. (2005)
7	British Columbia	Canada	49.9°N, 125.3°W	33	54	300	<i>Pseudotsuga menziesii</i> (Mirb.) Franco, <i>Thuja plicata</i> L., <i>Tsuga heterophylla</i>	1997–2005	-3.580	7.562	1369.1	9.9	Krishnan et al. (2009)
8	NewBrunswick-Nashwaak	Canada	46.5°N, 67.1°W	-	34	341	<i>Abies balsamea</i> (L.) Mill.	2003–2005	-1.628	5.297	1196.0	2.1	Xing et al. (2005)
9	Quebec old mature boreal forest	Canada	49.7°N, 74.3°W	20	120	382	<i>Picea mariana</i> (Mill.) Britton, Sterns & Poggenburg	2003–2005	-0.627	3.574	961.3	0.4	Bergeron et al. (2007)
10	Saskatchewan-old jack pine	Canada	53.9°N, 104.7°W	14	94	520	<i>Pinus banksiana</i> Lambert	1999–2005	-0.677	2.863	430.0	0.1	Howard et al. (2004)
11	Sodankylä	Finland	67.4°N, 26.6°E	14	-	180	<i>Pinus sylvestris</i> L.	2003–2007	0.137	2.103	499.0	-1.1	Aurela (2005)
12	Hyytiälä	Finland	61.8°N 24.3°E	15	46	185	<i>Pinus sylvestris</i> L.	1997–2007	-0.518	4.037	620.0	2.2	Ilvesniemi & Liu (2001)

NEE, net ecosystem exchange.

10°C. After comparing different means of temporal fitting (monthly, biweekly, annual periods), we decided to fit a single expression per site since the differences in the proportion of explained variance were not very large.

Gross ecosystem exchange was modeled using the photosynthesis models of Mäkelä *et al.* (1996, 2004). The present version uses the modifications of the model presented by Kolari *et al.* (2007) (with the exception of the small leaf respiration term, which we omitted). We also used an Arrhenius function for respiration instead of the exponential function used by Kolari *et al.* (2007). This model was originally developed for individual leaves but it was applied here as a big-leaf model. The use of a big-leaf version of this model is justified for atmospherically well-coupled canopies since responses of photosynthetic production to irradiance and vapor pressure are multiplicative. In the model, the gross photosynthetic rate $A(t)$ (in $\mu\text{mol CO}_2 \text{ m}^{-2} \text{ s}^{-1}$) was modeled as a nonlinear function of stomatal conductance of CO_2 $g(t)$ (in $\mu\text{mol CO}_2 \text{ m}^{-2} \text{ s}^{-1}$), photosynthetic capacity $\alpha(t)$ (in $\mu\text{mol CO}_2 \text{ m}^{-2} \text{ s}^{-1}$), and a saturation function of light intensity $\gamma(t)$ (dimensionless):

$$A(t) = \frac{g(t) \cdot C_a \cdot \alpha(t) \cdot \gamma(t)}{g(t) + \alpha(t) \cdot \gamma(t)} \quad \text{Eqn 2}$$

where the stomatal conductance is expressed as:

$$g(t) = \max\{0.00001, \tilde{g}(t)\},$$

$$\text{with } \tilde{g}(t) = \left(\sqrt{\frac{C_a \cdot 10^{-6} \cdot \lambda}{1.6 \cdot D(t)}} - 1 \right) \cdot \alpha(t) \cdot \gamma(t) \quad \text{Eqn 3}$$

with and the light response of biochemical reactions of photosynthesis:

$$\gamma(t) = \frac{Q(t)}{Q(t) + \delta} \quad \text{Eqn 4}$$

Some of these units are slightly changed compared with the original articles to match units frequently used with eddy-covariance data. C_a is the air CO_2 concentration in ppm, $Q(t)$ is the photosynthetically active radiation in $\mu\text{mol m}^{-2} \text{ s}^{-1}$, $D(t)$ is the water vapor pressure deficit in kPa, calculated using temperatures above the tree canopies, δ is the half saturation parameter of the light function ($\mu\text{mol m}^{-2} \text{ s}^{-1}$) and λ is a model parameter expressing the carbon required in the long term to sustain transpiration flow (in kPa) derived from an optimal regulation model of stomatal conductance (Berninger & Hari, 1993).

As mentioned earlier, photosynthetic capacity $\alpha(t)$ was modeled as a lagged function of temperature $S(t)$, following Kolari *et al.* (2007), which was based on Mäkelä *et al.*

(2004), assuming that $\alpha(t)$ is a sigmoid function of $S(t)$. This can be interpreted as the maximum Rubisco limited rate of carboxylation (Kolari *et al.*, 2007). $S(t)$ is a transformation of temperature. It reflects the fact that the photosystem is likely to respond to increasing daily temperatures in a delayed and smooth way in early spring. After comparing different relationships, we used a sigmoid expression based on the logistic function, following Kolari *et al.* (2007):

$$\text{with } \alpha(t) = \alpha_{\max} / (1 + \exp(b \cdot (S(t) - T_s))) \quad \text{Eqn 5}$$

$$\text{and, } S(t) \text{ from } \frac{dS(t)}{dt} = \frac{T_{\text{air}}(t) - S(t)}{\tau} \quad \text{Eqn 6}$$

$T_{\text{air}}(t)$, the measured air temperature ($^{\circ}\text{C}$) at time t , and α_{\max} ($\mu\text{mol m}^{-2} \text{ s}^{-1}$), b ($^{\circ}\text{C}^{-1}$), T_s ($^{\circ}\text{C}$) and τ are the model parameters: α_{\max} is the maximum photosynthetic efficiency; b is the curvature of the sigmoid function and T_s is the inflection point of the sigmoid curve, that is, the temperature at which α reaches half of α_{\max} ; and τ is the time constant (here shown in d) of photosynthetic acclimation and indicates the time it takes for photosynthetic capacity to acclimatize itself to changing temperature. Higher values correspond to longer periods of acclimation of the photosynthesis response to temperature change in the spring (for more details, see Mäkelä *et al.*, 2004). We solved the differential equation for S using the Euler integration algorithm with the same time step as the meteorological observations.

As already described, the parameter λ regulates the stomatal response to vapor pressure deficit and it would be expected to decrease with increasing soil water deficit. However, in a preliminary analysis (not shown) the model was not particularly sensitive to changes in λ . This parameter proved to be the least influential in the model fit and often it was difficult to estimate λ and the other parameters simultaneously from the CO_2 exchange measurements. Thus, to avoid parameter trade-offs in the system of nonlinear equations (Canham & Uriarte, 2006) and since we were most interested in studying the variability of τ and α_{\max} , we fixed λ at 3000 kPa and optimized the model for the other five parameters. Attempts to make stomatal conductance sensitive to soil water contents (by making λ sensitive to soil water content as in Mäkelä *et al.*, 1996 and Berninger *et al.*, 1996) did not improve the model fit (data not shown). Additionally, previous published studies as well as our own parameter estimation attempts (data not shown) showed that, with the soil moisture data available, soil moisture effects were generally not very important when estimating photosynthesis in boreal stands (Hollinger *et al.*, 2004; Mäkelä *et al.*, 2006, 2008a; Luysaert *et al.*, 2007; Vogel *et al.*, 2008), which supports the assumption of constant λ in our modeling approach. Therefore, we did not

include the effects of soil moisture on photosynthesis in the model.

Modeling approach

Several types of model, with different parameterization and including different datasets from the 12 sites studied, were compared. First, to study the variability of τ along a latitudinal and temperature gradient, we began by fitting the model to each of the 12 datasets analyzed (Table 1), to estimate the five parameters (τ , δ , α_{\max} , b , T_s) in 12 ‘best-fit models’ (Table 2). We investigated whether trends in latitude, NDVI (mostly as an indirect estimate of leaf area index and chlorophyll content; e.g. Gamon *et al.*, 1995), mean temperature, and maximum and minimum temperatures in April and May (both of the air and the soil) could explain the between-site variation in parameter values. NDVI was calculated for the period 9–25 June, for 2003 and 2004, as the mean pixel value included in the 250×250 m MODIS images (http://daac.ornl.gov/cgi-bin/MODIS/GR_col5_1/mod_viz.html).

Secondly, assuming a direct, rather than a delayed, response of photosynthetic capacity to temperature, the model was fitted to the 12 datasets to study the importance of the time delay in the acclimation of photosynthesis. Therefore, we refitted the model by replacing S in Eqn 5 with the air temperature T_{air} , as expressed in Eqn 6.

Thirdly, we studied how well the model could predict photosynthetic production of evergreen needle-leaf forest stands without prior knowledge of stand properties. This was done by evaluating the fit of the model after expressing the estimated parameters as a function of remotely sensed or climatically derived covariates (NDVI, mean air temperature, mean precipitation and latitude). We assumed that reorganization of the photosystem driven by temperature is likely to occur mainly during spring. Therefore, we established nonlinear relationships between the values of the parameters of the photosynthesis model and climatic variables both for the whole year and for April and May. More specifically, the variables we considered in spring were the mean daily minimum, the mean daily maximum, the mean daily temperature and the monthly temperature range in April and May. In addition, we fitted models to pooled data grouped in three different clusters of different ecology (see more details in the following sections and in Tables 3, 4).

The models were compared by commonly used goodness-of-fit statistics such as bias, absolute bias, root mean square error (RMSE) and the coefficient of determination (R^2). To distinguish between nonlinear regressions and linear regressions and the theoretical unsuitability of calculating R^2 in nonlinear models, we used the term efficiency (EF) to refer to proportion of explained variance (the analog of R^2) calculated for nonlinear models and R^2 to that

Table 2 Best-fit model results

#	Station	No. of observations	τ	δ	α_{\max}	b	T_s	Bias	RMSE	EF
1	NOBS	79 139	6.112 (0.002)	313.68 (2.025)	0.0581 (0.0001)	-0.2016 (< 0.0001)	6.689 (0.035)	0.0214	1.832	68.19
2	Harvard hemlock	10 045	1.049 (0.045)	489.60 (16.500)	0.0849 (0.0011)	-0.2906 (0.0081)	7.024 (0.111)	0.0654	3.264	72.43
3	Wind River	36 418	0.756 (0.056)	369.92 (11.457)	0.0625 (0.0007)	-0.4086 (0.0233)	2.255 (0.143)	0.0621	6.302	39.96
4	Niwot Ridge	158 528	3.129 (< 0.001)	285.62 (0.457)	0.0455 (< 0.0001)	-0.3007 (< 0.0001)	4.970 (0.001)	0.0450	1.856	69.09
5	Howland Forest	67 896	3.473 (0.061)	528.96 (6.606)	0.0845 (0.0004)	-0.2606 (0.0026)	7.216 (0.045)	0.1839	3.245	73.86
6	Sask-Black Spruce	71 735	4.283 (0.046)	771.38 (8.071)	0.0617 (0.0003)	-0.3733 (0.0035)	4.951 (0.027)	0.1595	1.662	76.30
7	British Columbia	55 412	0.017 (0.001)	261.43 (3.359)	0.096721 (0.00005)	-0.2011 (0.0037)	3.758 (0.080)	0.0249	4.326	71.78
8	NewBrun-Nashwaak	32 278	8.715 (0.250)	773.39 (15.259)	0.0869 (0.0008)	-0.2809 (0.0050)	3.142 (0.073)	-0.0231	2.738	73.10
9	Quebec mature boreal	23 641	1.160 (0.034)	410.53 (8.839)	0.0578 (0.0005)	-0.2698 (0.0051)	6.505 (0.088)	0.1638	2.145	65.12
10	Sask- old jack pine	50 445	6.596 (0.108)	845.78 (15.440)	0.0519 (0.0005)	-0.3216 (0.0047)	5.402 (0.054)	0.0950	1.794	61.68
11	Sodankyla	87 648	14.421 (0.165)	191.78 (2.061)	0.0359 (0.0002)	-0.2702 (0.0032)	5.870 (0.055)	0.0185	1.398	55.78
12	Hyytiälä	176 521	4.154 (< 0.001)	982.69 (1.660)	0.0990 (0.0002)	-0.2889 (< 0.0001)	5.028 (0.003)	-0.0973	1.596	84.56
	Mean		4.489	518.73	0.069	-0.289	5.234	0.060	2.68	67.65
	SD		4.0834	262.02	0.021	0.060	1.564	0.082	1.44	11.36
	Median		3.813	450.07	0.062	-0.285	5.215	0.054	2.00	70.44
	CV		90.99	50.51	30.23	20.76	29.89	136.50	53.74	16.80

Approximate standard errors of parameters are shown in parentheses. Mean bias and root mean square error (RMSE) are in $\mu\text{mol m}^{-2} \text{s}^{-1}$; τ is in $\mu\text{mol m}^{-2} \text{s}^{-1}$; δ is in $\mu\text{mol m}^{-2} \text{s}^{-1}$; α_{\max} in micromols $\text{m}^{-2} \text{s}^{-1}$; b in $^{\circ}\text{C}^{-1}$; T_s in $^{\circ}\text{C}$. EF, efficiency.

Table 3 Model parameters for different pooled datasets

# Model	No. of datasets	No. of fits	No. of observations	τ	δ	α_{\max}	b	T_s	Bias	RMSE	EF
1	North America, $T_{\text{mean}} < 2.5$	6	396 350	7.291 (< 0.001)	207.77 (0.201)	0.0437 (< 0.0001)	-0.2505 (< 0.0001)	4.934 (0.001)	0.129	2.144	63.45
2	North America, $T_{\text{mean}} > 2.5$	4	164 443	4.501 (0.072)	232.27 (2.561)	0.0651 (0.0002)	-0.4031 (0.0051)	3.911 (0.032)	0.073	5.454	45.33
3	North America, $T_{\text{mean}} > 2.5$ (-Wind River)	3	133 353	5.086 (0.210)	248.62 (2.342)	0.0752 (0.0002)	-0.3473 (0.0034)	4.633 (0.030)	0.041	4.650	58.10
4	Finland	2	263 967	8.333 (< 0.001)	240.12 (0.275)	0.0512 (< 0.0001)	-0.2998 (< 0.0001)	5.015 (0.001)	0.172	1.839	73.12
5	Boreal	12	824 760	5.206 (< 0.001)	390.69 (0.364)	0.0617 (< 0.0001)	-0.3001 (< 0.0001)	4.998 (0.001)	-0.001	3.268	51.68
6	Boreal (expanded parameters) ^a	12	792 482	^a	336.75 (0.274)	*	-0.3000	4.807 (< 0.001)	-0.060	3.081	57.04

^aExpanding: $\alpha_{\max} = 0.0061[0.0000]\exp(0.0003[0.0000]\text{NDVI}_{\text{June}})$; (SD between square brackets); $\tau = 6.239[\leq 0.001]\exp(-0.3003[0.0000]T_{\text{mean}})$.

Approximate standard error of estimates are shown between parenthesis. Mean bias and root mean square error (RMSE) are in $\mu\text{mol m}^{-2} \text{s}^{-1}$; τ is in d; δ is in $\mu\text{mol m}^{-2} \text{s}^{-1}$; α_{\max} in $\mu\text{mol m}^{-2} \text{s}^{-1}$; b in $^{\circ}\text{C}^{-1}$; T_s in $^{\circ}\text{C}$. EF, efficiency.

calculated in linear models (e.g. Gea-Izquierdo & Cañellas, 2009).

Results

The mean half-hourly NEE for a site was directly related to site mean annual temperature (EF = 0.865), showing that net forest C fixation increased with increasing air temperature. The 12 single model best fits for the studied datasets are shown in Fig. 1 and Table 2, and an independent fit to show the performance of the respiration submodel to all valid eddy flux data collected when photosynthetic active radiation < 5 $\mu\text{mol m}^{-2} \text{s}^{-1}$ is shown in Supporting Information, Table S1.

For models fitted individually to each site (Model 1), the model fit was unbiased and EF values were generally above 65% with the exception of the Wind River site. However, when attempting to fit a single model to the whole dataset, the results were not as good (Table 3), showing that we were not able to model interstand variation (see the Discussion section). Additionally, when utilizing the parameters estimated for this single model to fit the different datasets individually, the results were biased (Table 4), even if the average bias in the model fit approached zero. We also fitted models to three different groups with similar ecological conditions, namely North America, $T_{\text{mean}} < 2.5^{\circ}\text{C}$ (continental sites); North America, $T_{\text{mean}} > 2.5^{\circ}\text{C}$ (maritime sites); and the European boreal sites. When grouping, the model results were quite good for the 'continental' sites (i.e., using a single equation yielded a good fit, as shown in Table 3), accounting for > 65% of the variance of half-hourly measured C flux, although slightly biased (bias = $-0.163 \mu\text{mol m}^{-2} \text{s}^{-1}$).

When studying the distribution of the fitted parameters along the cited covariates, we observed that τ (Fig. 2) and α_{\max} (Fig. 3) were negatively correlated with temperature, both with mean annual air temperature and with minimum soil temperature in April. Latitude also showed a positive correlation with τ ($R^2 = 0.314$). All parameters included in Table 2 were significant, showing the sigmoid nature of photosynthesis capacity (parameters α_{\max} , b and T_s) and the significance of the delay parameter (τ).

As already stated, photosynthesis was modeled as a sigmoid function of the transformed temperature (Eqns 5, 6) depending on three parameters. The different values of b and T_s in the different best-fit models (Table 2) result in different shapes of the sigmoid response of photosynthetic capacity to temperature. The inflection point (T_s) is the temperature at which photosynthetic capacity reaches 50%, and we observed that this temperature was inversely related to mean temperature (Fig. 3b). Thus, high photosynthesis rates were achieved at higher temperatures at colder sites.

As expected, NDVI was strongly related to T_{mean} , mean NEE, annual precipitation in mm (P_{mm}), continentality and minimum soil temperature in April (Fig. 4a, and data

Table 4 Fit statistics for four scenarios: no delay (i.e. $S(t) = T_{\text{air}}$); statistics calculated using the parameters fitted for a single model to all datasets (model #5 Table 3, statistics calculated applying the parameters fit in model 5 from Table 3 independently to the datasets, then calculating the fit statistics; this being the reason for the small difference with Table 3); and best fit models (from Table 2) for comparison purposes

#	Model	# datasets	# fits	Bias		RMSE		EF		Bias	
				Mean	SD	Mean	SD	Mean	SD	Mean	SD
1	No delay	12	12	-0.015	0.083	2.834	1.376	62.787	11.610	0.069	0.044
2	All fixed	12	-	-0.285	1.740	3.100	1.677	52.823	24.495	0.916	1.484
3	Best fit	12	12	0.060	0.082	2.680	1.440	67.654	11.365	0.080	0.060

Bias and root mean square error (RMSE) are in $\mu\text{mol m}^{-2} \text{s}^{-1}$. EF, efficiency.

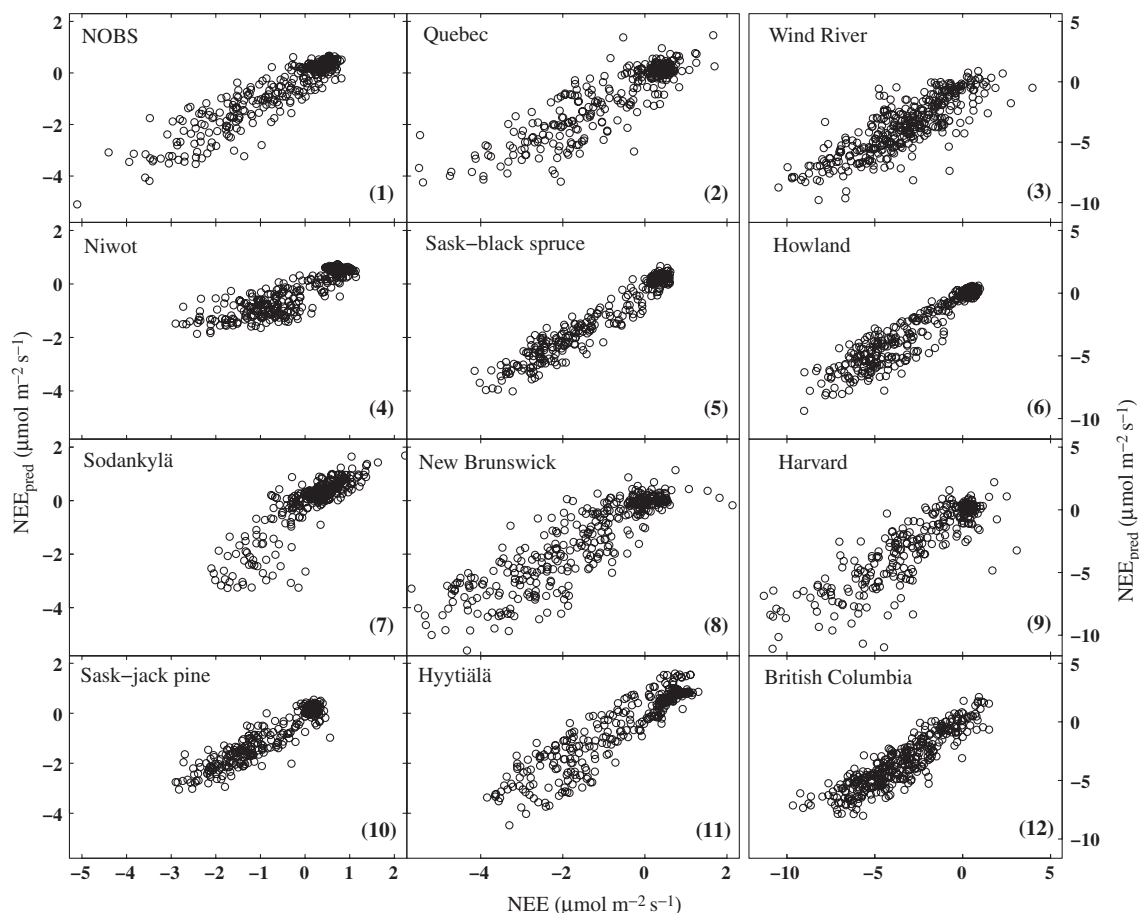


Fig. 1 Scatter plots of predicted daily averages (2000–2005, nongap-filled data) for the 12 datasets. Datasets are described in Table 1. NEE, net ecosystem exchange.

not shown). NDVI also had a high correlation with asymptotic photosynthetic capacity (Fig. 4b). The model fit got much worse when we replaced the delayed temperature response with an immediate response (this was done by setting $S(t) = T_{\text{air}}(t)$) (Table 4). Furthermore, the significant model error increased and efficiency decreased when fixing $S(t) = T_{\text{air}}(t)$. The importance of the delayed temperature response for the model fit was higher for sites with cold springs, but relatively minor at some of the warmer maritime sites (Fig. 5). The influence of the parameter τ on

photosynthetic capacity and NEE estimations can be better observed in Fig. 6. Higher values of τ decrease and smooth the transformed temperature used for NEE calculations. In Fig. 6(d), we illustrate model behavior for different values of τ , showing the response of photosynthetic capacity to a step change in temperature: for a tree with an instantaneous response to temperature (low τ), the response of photosynthesis to temperature changes will be very fast, whereas for a tree with a typical value of τ for a boreal conifer forest (suggested by our results as $\tau = 6.1$ d) it would take > 1 wk

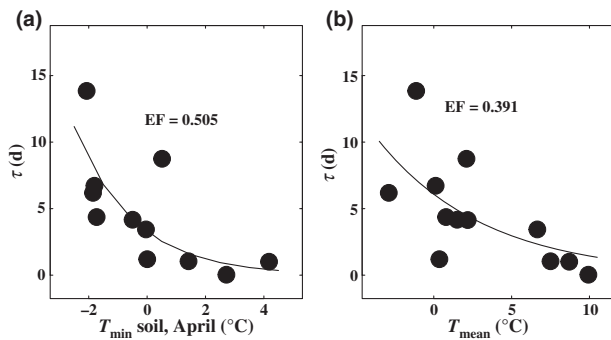


Fig. 2 Relationships between acclimation parameter (τ) from best-fit models (presented in Table 2) and minimum soil temperature ($^{\circ}\text{C}$) in April (a) and site mean annual temperature (b). EF, efficiency.

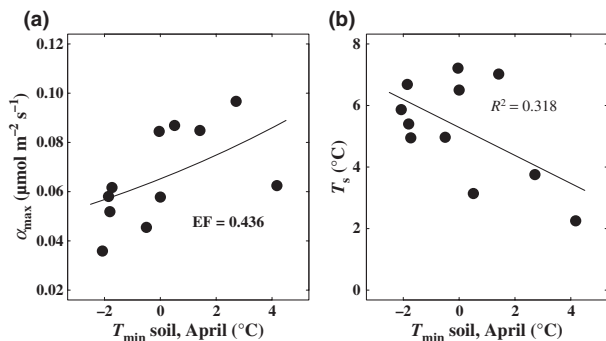


Fig. 3 Distribution of photosynthetic capacity parameters as estimated in best-fit models (Table 2) as a function of minimum April soil temperature: (a) maximum photosynthetic capacity (α_{max}); (b) temperature inflection point (T_s , 50% photosynthetic capacity). EF, efficiency.

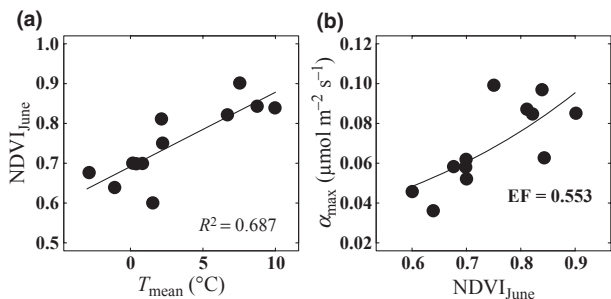


Fig. 4 (a) Relationship between normalized difference vegetation index (NDVI) and annual mean temperature (a) and maximum photosynthetic capacity (α_{max}) (b) estimated in best-fit models (Table 2) as a function of NDVI.

for photosynthesis to reach its new value. In reality, when temperature changes more gradually, the results are less dramatic, but important differences in the behavior of photosynthesis existed during springtime (Fig. 6).

Discussion

Photosynthesis in conifer forests from colder sites responded more slowly to temperature than in warmer

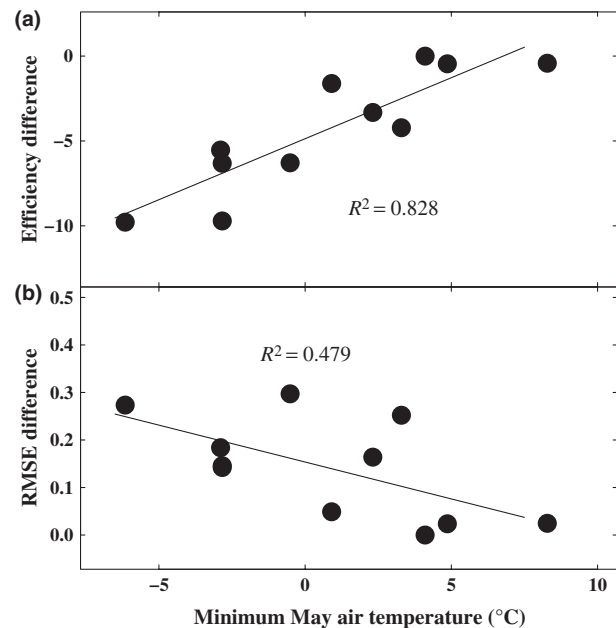


Fig. 5 (a) Difference between model efficiency (EF) calculated for the best-fit lagged model (as from Table 2) and the nonlag (i.e. $S(t)=T_{\text{air}}$) model (i.e. $\text{EF}_0 - \text{EF}_{\text{best}}$) as a function of the minimum May air temperature for the study sites ($n = 11$); (b) as (a), but for the difference of root mean square error (RMSE) between the two models (i.e. $\text{RMSE}_0 - \text{RMSE}_{\text{Best}}$).

forests situated further south. The simple model used explained well the intra- and interannual variation of NEE and photosynthetic capacity in evergreen boreal needle-leaf forests of the northern hemisphere and exhibited a very good fit to the data from 12 different cool temperate and boreal evergreen coniferous forests, as did previous similar approaches (e.g. Mäkelä *et al.*, 2004, 2008a). The goodness-of-fit statistics are similar to those observed in more complex modeling approaches (Yuan *et al.*, 2008). Parsimony is one of the most desirable characteristics in any model. The greater the simplicity of a model, the easier it is to achieve a good comparison of parameters, since trade-offs between parameters (Canham & Uriarte, 2006) are more likely to be avoided.

The use of a time-delayed model improved the fit of the model, particularly for the boreal locations considered. The values of τ increased from warm to cold sites, indicating that the response of photosynthesis to temperature changes in these colder sites is slower. Since, in addition, the growing season in these areas is shorter, the importance of the time constant in the estimation of the whole growing season C balance increased (Figs 2, 5). When we modeled photosynthesis as an instant (with no time delay) response to temperature, the goodness of fit decreased in the northern sites, whereas the fit remained unchanged for warmer maritime sites (Fig. 5). This indicates that, in cold boreal climates, slow changes in photosynthetic capacity must be modeled

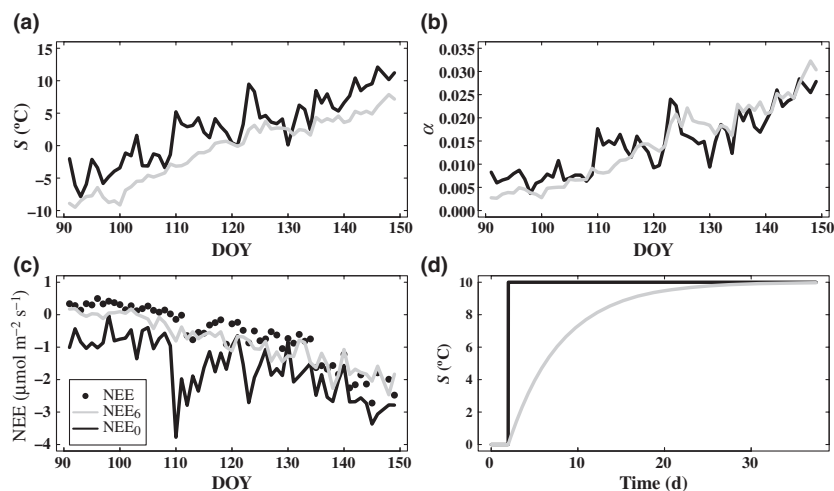


Fig. 6 Comparison of spring (April–May) 2000 results for NOBS model using a direct response to temperature and using the acclimation model with $\tau = 6.1$ d (S_6): (a) average daily S and temperature (i.e. S_0) as a function of Day of the Year (DOY) (S_0 , black line; S_6 , grey line); (b) photosynthetic capacity as a function of DOY (α_0 , black line; α_6 , grey line), (c) average net ecosystem exchange (NEE) (dots are observed NEE, lines are estimated NEE) as a function of DOY; (d) conceptual outline of the model response to a sudden change in 10°C if temperature was kept constant, when coming from the same state $S = 0^\circ\text{C}$ for models using $S(t) = T_{\text{air}}$ and $\tau = 6.1$ d (S_0 , black line; S_6 , grey line). Subindices 0 and 6 correspond to models fitted with $S(t) = T_{\text{air}}$ (i.e. $\tau = 0.0$) and $\tau = 6.1$ d, respectively.

to correctly estimate forest productivity and C balances. Mäkelä *et al.* (2008a) obtained similar results on a smaller dataset.

The temperatures at which photosynthetic capacity acclimatizes to 50% of its maximum value at the different sites were between 2 and 8°C (Fig. 3), indicating that photosynthetic capacity increases rapidly above 0°C . Similarly to acclimation temperature, at cold sites the temperature at which photosynthesis was saturating (i.e. approaching α_{max}) also seemed higher than at warmer sites (Fig. 3). Plant physiologists have argued that photosynthetic responses of C_3 plants to temperature should be very similar, although this idea continues to be challenged, since genetically different versions of Rubisco seem to have different temperature responses (Sage, 2002). While low temperatures as such do not necessarily harm the photosystem, conditions that combine high light with cold temperatures are known to be detrimental to the photosynthetic apparatus. High light and low temperature generate an imbalance between the light and the dark reactions of photosynthesis, and excess excitation energy may damage the photosystem. Boreal conifers react to these conditions by disassembling their photosystems and by protecting themselves with the creation of alternative electron sinks, mainly xanthophylls. How strongly the photosystem is disassembled seems to depend on temperature and light availability (Slot *et al.*, 2005; Porcar-Castell *et al.*, 2008).

Most studies modeling the recovery of photosynthesis in the spring have used air temperature as the primary determinant of photosynthetic recovery (Pelkonen & Hari, 1980; Mäkelä *et al.*, 2004). It has been argued that both air and soil temperatures are likely to be major limiting factors

that affect the recovery of photosynthetic capacity in the spring, and this also seems to be reflected in our results. Controlled-environment studies have consistently shown that low soil temperatures decrease the rate of photosynthesis of seedlings (Vapaavuori *et al.*, 1992). However, for large trees, the evidence concerning the effects of soil temperature on photosynthetic capacity is less clear. Most recent experimental studies show that photosynthesis of large trees in spring is probably not very sensitive to increases in the soil temperature, although decreases in soil temperature tend to slow down the recovery process (Bergh & Linder, 1999; Strand *et al.*, 2002). Nevertheless, Suni *et al.* (2003b) showed that some photosynthesis occurs when soils are still at 0°C and the stem contains a large, partially accessible, water reservoir that trees can utilize for photosynthesis in the spring (Running, 1980).

The modeled photosynthetic capacity (α_{max}) showed a high correlation with NDVI, which is usually a good indicator of the photosynthetic capacity of plant canopies (Gamon *et al.*, 1995) and has been directly related to CO_2 flux measurements (Yuan *et al.*, 2007; Lindroth *et al.*, 2008). Using NDVI to expand the photosynthetic capacity improved the goodness in a single model fit for all data (Table 3), although the behavior was significantly worse than fitting the model separately to each of the sites studied. Probably a greater number of locations would help to improve the relationship between parameters and covariates. Factors such as precipitation, temperature and NDVI are correlated among themselves. Thus it is not possible to fully quantify their individual importance. Other studies with different approaches have also reported good fits for pooled expanded models for several locations, especially for daily

and monthly time-lags (Bergeron *et al.*, 2007; Mäkelä *et al.*, 2008a). This lack of fit was probably not the result of between-species differences. For example, the North American sites with a mean annual temperature below 2.5°C (as suggested by our data) behaved very similarly (regardless of the species within *Picea* sp., *Pinus* sp. and *Abies* sp. (Table 1)) according to the fitted model (Table 3).

The measured average NEE became more negative with increasing mean site temperature, similar to previous studies (e.g. Valentini *et al.*, 2000; Lindroth *et al.*, 2008). The northernmost forests were almost C-neutral, while more southern forests were C sinks (Table 1). The modeled photosynthetic capacity increased with site mean temperature and minimum temperatures in early April (Figs 3, 4). The model fit was the poorest at the Wind River site, the oldest, rainiest and second warmest forest, and hence with different ecology (maritime humid conifer forest with summer drought (Falk *et al.*, 2005, 2008)). This could be related to estimation of respiration in an old stand (Table S1; Falk *et al.*, 2005, 2008; Lindroth *et al.*, 2008) as well as moisture limitations not included in the model and likely to be more influential in that site compared with pure boreal stands (Reichstein *et al.*, 2007; Falk *et al.*, 2008). Respiration is not a straightforward process to estimate, since it is known to be influenced by several different factors difficult to quantify, such as climate or forest stand attributes, that will affect future flux estimations (e.g. Lloyd & Taylor, 1994; Xu *et al.*, 2004).

Further extensions of this analysis could be in studying the effect of foliar nitrogen concentrations on net C exchange (Mäkelä *et al.*, 2008a; Ollinger *et al.*, 2008) or examining the influence of some other factors that were not included in the present model, such as shading, and by including absorbed radiation rather than incoming photosynthetic active radiation as drivers of the model. It would also be interesting to expand the model to nonboreal forests where soil moisture is more limiting, as this has been shown to affect photosynthesis and C allocation in some ecosystems (e.g. Reichstein *et al.*, 2007; Falk *et al.*, 2008).

The temporal and spatial variability of photosynthetic production and C exchange over large areas is important for global models of the C cycle and the prediction of the impacts of climate change. The length of the photosynthetically active period is an important determinant of annual photosynthetic production in boreal, alpine and temperate ecosystems (e.g. Suni *et al.*, 2003a; Baldocchi *et al.*, 2005). Forests in colder northern areas seem to be slower in adapting their photosynthetic capacity to changes in air temperature. We do not know if these differences between sites are genetically or environmentally determined. In this paper, we show that a simple temperature-driven model of the phenology of photosynthesis predicts well the development of photosynthetic capacity through time. Failure to do so will lead to important overestimations of photosynthetic production (Berninger, 1997; Bergh & Linder 1999).

Acknowledgements

This contribution was partly funded by a NSERC strategic grant held by Y.B. and F.B. We thank the participants and supporters of Ameriflux, Fluxnet and the Canadian Carbon Program (CFCAS, NSERC, NRCAN, Environment Canada) for providing the flux and meteorological data. The Howland research was supported by the Office of Science (BER), US Department of Energy, Interagency Agreement No. DE-AI02-07ER64355.

References

- Aurela M. 2005. *Carbon dioxide exchange in subarctic ecosystems measured by a micrometeorological technique*. PhD thesis, Finnish Meteorological Institute Contributions. URL <http://ethesis.helsinki.fi/julkaisut/mat/fysik/vk/aurela/> [last accessed 6 July 2010].
- Baldocchi DD. 2003. Assessing the eddy covariance technique for evaluating carbon dioxide exchange rates of ecosystems: past, present and future. *Global Change Biology* 9: 479–492.
- Baldocchi DD, Black TA, Curtis PS, Falge E, Fuentes JD, Granier A, Gu L, Knohl A, Pilegaard K, Schmid HP *et al.* 2005. Predicting the onset of net carbon uptake by deciduous forests with soil temperature and climate data: a synthesis of FLUXNET data. *International Journal of Biometeorology* 49: 377–387.
- Bergeron O, Margolis HA, Black TA, Coursolle C, Dunn AL, Barr AG, Wofsy SC. 2007. Comparison of carbon dioxide fluxes over three boreal black spruce forests in Canada. *Global Change Biology* 13: 89–107.
- Bergh J, Linder S. 1999. Effects of soil warming during spring on photosynthetic recovery in boreal Norway spruce stands. *Global Change Biology* 5: 245–253.
- Berninger F. 1997. Effects of drought and phenology on GPP in *Pinus sylvestris*: a simulation study along a geographical gradient. *Functional Ecology* 11: 33–42.
- Berninger F, Hari P. 1993. Optimal regulation of gas exchange evidence from field data. *Annals of Botany* 71: 135–140.
- Berninger F, Makela A, Hari P. 1996. Optimal control of gas exchange during drought: empirical evidence. *Annals of Botany* 77: 469–476.
- Black TA, Gaumont-Guay D, Jassal RS, Amiro BD, Jarvis PG, Gower ST, Kelliher FM. 2005. Measurement of CO₂ exchange between boreal forest and the atmosphere. In: Griffiths H, Jarvis PJ, eds. *The carbon balance of forest biomes*. New York, NY, USA: Taylor and Francis Group, 151–186.
- Canham CD, Uriarte M. 2006. Analysis of neighborhood dynamics of forest ecosystems using likelihood methods and modeling. *Ecological Applications* 16: 62–73.
- D'Arrigo RD, Kaufmann RK, Davi N, Jacoby GC, Laskowski C, Myneni RB, Cherubini P. 2004. Thresholds for warming-induced growth decline at elevational tree line in the Yukon Territory, Canada. *Global Biogeochemical Cycles* 18, GB3021: doi: 10.1029/2004GB002249.
- Dunn AL, Barford CC, Wofsy SC, Goulden ML, Daube BC. 2007. A long-term record of carbon exchange in a boreal black spruce forest: means, responses to interannual variability, and decadal trends. *Global Change Biology* 13: 577–590.
- Ensminger I, Sveshnikov D, Campbell D, Funk C, Jansson S, Lloyd J, Shibistova O, Öquist G. 2004. Intermittent low temperatures constrain spring recovery of photosynthesis in boreal Scots pine forests. *Global Change Biology* 10: 995–1008.
- Falge E, Baldocchi D, Olson R, Anthoni P, Aubinet M, Bernhofer C, Burba G, Ceulemans R, Clement R, Dolman H *et al.* 2001. Gap filling strategies for defensible annual sums of net ecosystem exchange. *Agricultural and Forest Meteorology* 107: 43–69.

- Falk M, Paw U KT, Wharton S, Schroeder M. 2005. Is soil respiration a major contributor to the carbon budget within a Pacific Northwest old-growth forest? *Agricultural and Forest Meteorology* 135: 269–283.
- Falk M, Wharton S, Schroeder M, Ustin S, Paw U KT. 2008. Flux partitioning on an old growth forest. *Tree Physiology* 28: 509–520.
- Friend AD, Arneth A, Kiang NY, Lomas M, Ogee J, Rodenbeck C, Running SW, Santaren JD, Sitch S, Viovy N *et al.* 2007. FLUXNET and modelling the global carbon cycle. *Global Change Biology* 13: 610–633.
- Gamon JA, Field CB, Goulden ML, Griffin KL, Hartley AE, Joel G, Peñuelas J, Valentini R. 1995. Relationships between NDVI, canopy structure, and photosynthesis in three Californian vegetation types. *Ecological Applications* 5: 28–41.
- Gea-Izquierdo G, Cañellas I. 2009. Analysis of holm oak intraspecific competition using Gamma regression. *Forest Science* 55: 310–322.
- Goulden ML, Winston GC, Mcmillan AVS, Litvak ME, Read EL, Rocha AV, Elliot JR. 2006. An eddy covariance mesonet to measure the effect of forest age on land–atmosphere exchange. *Global Change Biology* 12: 2146–2162.
- Hadley JL, Schedlbauer JL. 2002. Carbon exchange of an old-growth eastern hemlock (*Tsuga canadensis*) forest in central New England. *Tree Physiology* 22: 1079–1092.
- Hollinger DY, Aber J, Dail B, Davidson EA, Goltz SM, Hughes H, Leclerc MY, Lee JT, Richardson AD, Rodrigues C *et al.* 2004. Spatial and temporal variability in forest-atmosphere CO₂ exchange. *Global Change Biology* 10: 1689–1706.
- Hollinger DY, Goltz SM, Davidson EA, Lee JT, Tu K, Valentine HT. 1999. Seasonal patterns and environmental control of carbon dioxide and water vapour exchange in an ecotonal boreal forest. *Global Change Biology* 5: 891–902.
- Howard EA, Gower ST, Foley JA, Kucharik CJ. 2004. Effects of logging on carbon dynamics of a jack pine forest in Saskatchewan, Canada. *Global Change Biology* 10: 1267–1284.
- Ilvesniemi H, Liu C. 2001. Biomass distribution in a young Scots pine stand. *Boreal Environment Research* 6: 3–8.
- Kolari P, Lappalainen HK, Hänninen H, Hari P. 2007. Relationship between temperature and the seasonal course of photosynthesis in Scots pine at northern timberline and in southern boreal zone. *Tellus. Series B, Chemical and Physical Meteorology* 59: 542–552.
- Krishnan P, Black TA, Jassal RS, Chen B, Nesic Z. 2009. Interannual variability of the carbon balance of three different-aged Douglas-fir stands in the Pacific Northwest. *Journal of Geophysical Research*. doi: 10.1029/2008JG000912.
- Lindroth A, Lagergren F, Aurela M, Bjarnadottir B, Christensen T, Dellwik E, Grelle A, Ibrom A, Johansson T, Lankreijer H *et al.* 2008. Leaf area index is the principal scaling parameter for both gross photosynthesis and ecosystem respiration of Northern deciduous and coniferous forests. *Tellus. Series B, Chemical and Physical Meteorology* 60B: 129–142.
- Linkosalo T. 1999. Regularities and patterns in the spring phenology of some boreal trees. *Silva Fennica* 33: 237–245.
- Lloyd J, Taylor JA. 1994. On the temperature dependence of soil respiration. *Functional Ecology* 8: 315–323.
- Luyssaert S, Janssens IA, Sulkava M, Papale D, Dolman AJ, Reichstein M, Hollmen J, Martin JG, Suni T, Vesala T *et al.* 2007. Photosynthesis drives anomalies in net carbon-exchange of pine forests at different latitudes. *Global Change Biology* 13: 2110–2127.
- Mäkelä A, Berninger F, Hari P. 1996. Optimal control of gas exchange during drought: theoretical analysis. *Annals of Botany* 77: 461–467.
- Mäkelä A, Hari P, Berninger F, Hänninen H, Nikinmaa E. 2004. Acclimation of photosynthetic capacity in Scots pine to the annual cycle of temperature. *Tree Physiology* 24: 369–376.
- Mäkelä A, Kolari P, Karimäki J, Nikinmaa E, Perämäki M, Hari P. 2006. Modelling five years of weather-driven variation of GPP in a boreal forest. *Agricultural and Forest Meteorology* 139: 382–398.
- Mäkelä A, Pulkkinen M, Kolari P, Lagergren F, Berbigier P, Lindroth A, Loustau D, Nikinmaa E, Vesala T, Hari P. 2008a. Developing an empirical model of stand GPP with the LUE approach: analysis of eddy covariance data at five contrasting conifer sites in Europe. *Global Change Biology* 14: 92–108.
- Mäkelä A, Valentine HT, Helmisaari HS. 2008b. Optimal co-allocation of carbon and nitrogen in a forest stand at steady state. *New Phytologist* 180: 114–123.
- Monson RK, Turnipseed AA, Sparks JP, Harley PC, Scott-Denton LE, Sparks K, Huxman TE. 2002. Carbon sequestration in a high-elevation, subalpine forest. *Global Change Biology* 8: 459–478.
- Morales P, Sykes MT, Prentice IC, Smith P, Smith B, Bugmann H, Zierl B, Friedlingstein P, Viovy N, Sabate S *et al.* 2005. Comparing and evaluating process-based ecosystem model predictions of carbon and water fluxes in major European forest biomes. *Global Change Biology* 11: 2211–2233.
- Myneni RB, Keeling CD, Tucker CJ, Asrar G, Nemani RR. 1997. Increased plant growth in the northern latitudes from 1981 to 1991. *Nature* 386: 698–702.
- Ollinger SV, Richardson AD, Martin ME, Hollinger DY, Frolking SE, Reich PB, Plourde LC, Katul GG, Munger JW, Oren R. *et al.* 2008. Canopy nitrogen, carbon assimilation, and albedo in temperate and boreal forests: functional relations and potential climate feedbacks. *Proceedings of the National Academy of Sciences, USA* 105: 19336–19341.
- Pelkonen P, Hari P. 1980. The dependence of the spring time recovery of CO₂ uptake in Scots pine on temperature and internal factors. *Flora* 169: 398–404.
- Porcar-Castell A, Juurola E., Ensminger I, Berninger F, Hari P, Nikinmaa E. 2008. Seasonal acclimation of photosystem II in *Pinus sylvestris*. II. Using the rate constants of sustained thermal energy dissipation and photochemistry to study the effect of the light environment. *Tree Physiology* 28: 1483–1491.
- Reichstein M, Falge E, Baldocchi D, Papale D, Aubinet M, Berbigier P, Bernhofer C, Buchmann N, Gilmanov T, Granier A. *et al.* 2005. On the separation of net ecosystem exchange into assimilation and ecosystem respiration: review and improved algorithm. *Global Change Biology* 11: 1424–1439.
- Reichstein M, Papale D, Valentini R, Aubinet M, Bernhofer C, Knohl A, Laurila T, Lindroth A, Moors E, Pilegaard K *et al.* 2007. Determinants of terrestrial ecosystem carbon balance inferred from European eddy covariance flux sites. *Geophysical Research Letters* 34: L01402. doi: 10.1029/2006GL027880.
- Running SW. 1980. Relating plant capacitance to the water relations of *Pinus contorta*. *Forest Ecology and Management* 24: 237–252.
- Sage RF. 2002. Variation in the k_{cat} of Rubisco in C₃ and C₄ plants and some implications for photosynthetic performance at high and low temperature. *Journal of Experimental Botany* 53: 609–620.
- Slot M, Wirth CH, Schumacher J, Mohren GMJ, Shibistova O, Lloyd J, Ensminger I. 2005. Regeneration patterns in boreal Scots pine glades linked to cold-induced photoinhibition. *Tree Physiology* 25: 139–1150.
- Strand M, Lundmark T, Soderbergh I, Mellander PE. 2002. Impacts of seasonal air and soil temperatures on photosynthesis in Scots pine trees. *Tree Physiology* 22: 839–847.
- Suni T, Berninger F, Markkanen T, Keronen P, Rannik Ü, Vesala T. 2003a. Interannual variability of growing-season timing, length, and CO₂ exchange in a boreal forest. *Journal of Geophysical Research* 108: 4265. doi: 2002JD002381.
- Suni T, Berninger F, Vesala T, Markkanen T, Hari P, Mäkelä A, Ilvesniemi H, Hänninen H, Nikinmaa E, Huttula T *et al.* 2003b. Air

- temperature triggers the commencement of evergreen boreal forest photosynthesis in spring. *Global Change Biology* 9: 1410–1426.
- Thum T, Aalto T, Laurila T, Aurela M, Hatakka J, Lindroth A, Vesala T. 2009. Spring initiation and autumn cessation of boreal coniferous forest CO₂ exchange assessed by meteorological and biological variables. *Tellus. Series B, Chemical and Physical Meteorology* 61: 701–717.
- Thum T, Aalto T, Laurila T, Aurela M, Lindroth A, Vesala T. 2008. Assessing seasonality of biochemical CO₂ exchange model parameters from micrometeorological flux observations at boreal coniferous forest. *Biogeosciences* 5: 1625–1639.
- Vaganov E, Hughes M, Kirilyanov A, Schweingruber FH, Silkin PP. 1999. Influence of snowfall and melt timing on tree growth on tree growth on subarctic Eurasia. *Nature* 400: 149–151.
- Valentini R, Matteucci G, Dolman AJ, Schulze ED, Rebmann C, Moors EJ, Granier A, Gross P, Jensen NO, Pilegaard K *et al.* 2000. Respiration as the main determinant of carbon balance in European forests. *Nature* 404: 861–865.
- Vapaavuori EM, Rikala R, Ryyppö A. 1992. Effects of root temperature on growth and photosynthesis on conifer seedlings during shoot elongation. *Tree Physiology* 10: 217–230.
- Vogel JG, Bond-Lamberty BP, Schuur EAG, Gower ST, Mack MC, O'Connell KEB, Valentine DW, Ruess RW. 2008. Carbon allocation in boreal black spruce forests across regions varying in soil temperature and precipitation. *Global Change Biology* 14: 1503–1516.
- Xing Z, Bourque C A, Clowater WC, Krasowski M, Meng F-R. 2005. Carbon and biomass partitioning in balsam fir (*Abies balsamea* (L.) Mill.). *Tree Physiology* 25: 1207–1217.
- Xu L, Baldocchi DD, Tang J. 2004. How soil moisture, rain pulses, and growth alter the response of ecosystem respiration to temperature. *Global Biogeochemical Cycles* 18: 1–10.
- Yuan FM, Arain MA, Barr AG, Black TA, Bourque CPA, Coursolle C, Margolis HA, McCaughey JH, Wofsy SC. 2008. Modeling analysis of primary controls on net ecosystem productivity of seven boreal and temperate coniferous forests across a continental transect. *Global Change Biology* 14: 1765–1784.
- Yuan W, Liu S, Zhou G, Tieszen LL, Baldocchi D, Bernhofer C, Gholz H, Goldstein AH, Goulden ML, Hollinger DY *et al.* 2007. Deriving a light use efficiency model from eddy covariance flux data for predicting daily gross primary production across biomes. *Agricultural and Forest Meteorology* 143: 189–207.

Supporting Information

Additional supporting information may be found in the online version of this article.

Table S1 Respiration goodness-of-fit statistics calculated for the different eddy-covariance sites (photosynthetically active radiation (PAR) < 5 $\mu\text{mol m}^{-2} \text{s}^{-1}$ or net ecosystem exchange (NEE) < 0)

Please note: Wiley-Blackwell are not responsible for the content or functionality of any supporting information supplied by the authors. Any queries (other than missing material) should be directed to the *New Phytologist* Central Office.